DEVELOPMENT OF TM$_{01}$ TO TE$_{11}$ CYLINDRICAL SWG MODE CONVERTER

During recent years, HPM systems are applied in various civilian, communication, space and defence applications. Furthermore, the remaining challenges are confronting the peak power radiation in the direction of propagation. This enables the HPM systems utility in solar power microwave transmission through space to ground and in space beam driven rocket [Benford *et al.* (2007)]. Most of the HPM sources generate azimuthally symmetrical mode TM_{01} and *TEM*. Direct radiation of TM_{01} mode using horn antenna provides null along the boresight in the far-field region. To avoid this null at the boresight, the TM_{01} mode is required to convert in the TE_{11} mode before radiating, using the mode converter.

Conventional serpentine, dual-bend, and shorted coaxial rectangular waveguides are used to design the TM_{01} to TE_{11} mode converter, but such structures are complicated in design and fabrication [Yang *et al.* (1995), Ling and Zhou (2001), Yang *et al.* (1995) and Lee *et al.* (2004)]. Sectoral waveguide mode converter has an advantage of simplified design and easier fabrication [Somov *et al.* (1998) and Yuan *et al.* (2005)]. Also, this design can support high power microwave but such mode converters are bulky since they are all metal structure with a coaxial cylinder. Also, it requires an additional section to convert TM_{01} mode to *TEM* mode, which further increases its weight and complexity in design. The tapered metallic baffle mode converter is a light weight structure along with of having low return loss [Chittora *et al.* (2015)]. Dielectrically loaded mode converter has been reported with high conversion efficiency [Chittora *et al.* (2015)]. But such mode converter contains lot of dielectric material and is more sensitive at higher temperature, which leads to thermal expansion, deformation as well as RF losses.

Mode converter with lesser in weight, linear in structure and HPM sustainable design can be achieved by using cylindrical sectoral waveguide (CSWG). Therefore,

all-metal lightweight CSWG mode converter structure with low loss, high efficiency and the high power handling capability is reported in this Chapter, used for converting TM_{01} to TE_{11} mode. This mode converter is linear in design, all metal, light weight and compact structure, and easier in fabrication.

5.1. CSWG Design and Development

Proposed cylindrical sectoral mode converter is made of metallic plates by inserting them in a circular waveguide, as shown in Figure 5.1. In this mode converter, axial-azimuthal metallic plates are used to separate circular waveguide in many CSWG [Elsherbeni *et al.* (1991)]. Region *I* contain TM_{01} mode radiated from mode launcher. In Region *II*, metal plates start with tapered metallic plates to reduce reflections to a negligible value. In Region *III*, three CSWGs are having azimuthal angle π radian (for one sector) and $\pi/2$ radian (for two sectors) are represented throughout this chapter as CSWG$_\pi$, and CSWG$_{\pi/2}$, respectively. By introducing using π phase delay, between lower (two CSWG$_{\pi/2}$) and upper (CSWG$_\pi$) part of Region *III*, the orientation of TE_{11} mode become similar to both sectors at the end of this region. In order to obtain the π phase delay, the length of the metal plate is calculated using the following relationship:

$$L = \frac{\pi}{\beta_1 - \beta_2} \tag{5.1}$$

where L is the length of Region *III*, also β_1 and β_2 are the axial propagation constants for CSWG$_\pi$ and CSWG$_{\pi/2}$ sections, respectively. Due to different circular sectoral waveguide impedances in Region *III*, the field content in lower (two CSWG$_{\pi/2}$) and upper (CSWG$_\pi$) would be mismatched and disbalanced. Thus, the output beam in the TE_{11} mode is also unstable. To stabilize the output beam an extra region is added is region *IV*, where a tapered plated is helping to synchronise field orientation of lower sectoral region field with upper sectoral region field.
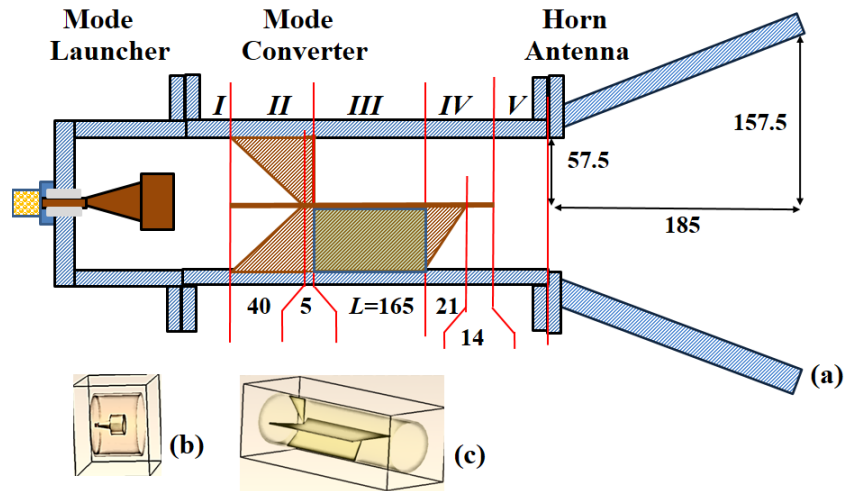
Figure 5.1. (a) Design of a cylindrical sectoral waveguide mode converter for TM_{01} to TE_{11}, and all parameters in mm. **(b)** 3D model of mode launcher and **(c)** mode converter.
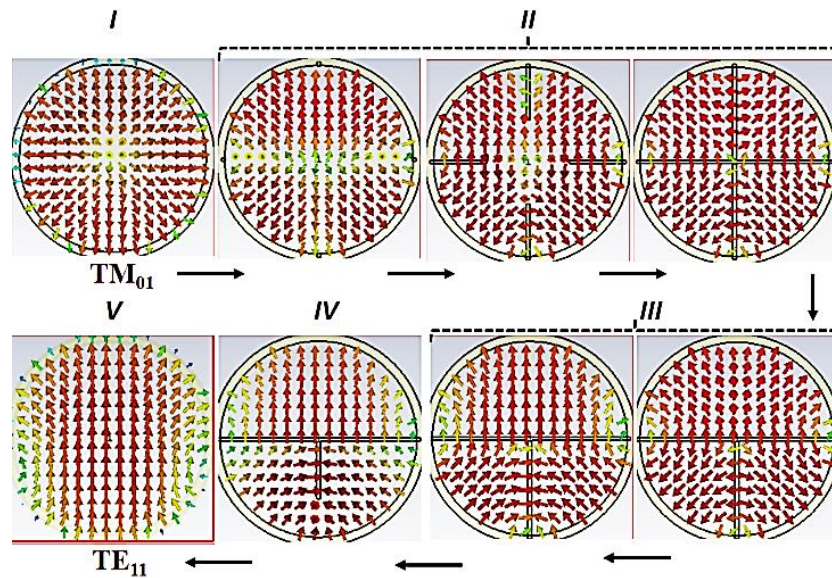

Figure 5.2. The process of mode conversion demonstrated using the electric field at a different axial position in the cylindrical sectoral waveguide mode converter for TM_{01} to TE_{11} mode.

The simulated electric field over the apertures at each junction are exhibited in Figure 5.2, to understand the operating principle. The TM_{01} mode is fed to the cylindrical waveguide in region *I*. By introducing tapered metallic plates in Region *II*, TM_{01} mode of the cylindrical waveguide is converted into the TE_{11} mode of all CSWG. These tapered structures are similar to the tapered resistive card of the Rotatory vane type

attenuator, used to reduce the reflections (Collin *et al.* 2005). The orientation of electric field lines, in the input side of Region *III*, between $CSWG_\pi$ and $CSWG_{\pi/2}$ is π rad. As the field pattern introduce π phase difference between $CSWG_\pi$ and $CSWG_{\pi/2}$ due to axial length (*L*) of the Region *III*, the electric field will meet in the same orientation at the output end. This results in the field pattern of the TE_{11} mode in a cylindrical waveguide.

5.2. Experimental Setup

The proposed CSWG mode converter is fabricated and low power experiments are performed for the conversion of TM_{01} to TE_{11} mode. Since there is no dedicated device to distinguish the converted mode, so the mode is identified by comparing the far-field radiation pattern. Therefore, to measure the far-field radiation pattern antenna measurement setup is shown in Figure 5.3. The distance between two antennas is kept 2000 mm apart and the gain of receiving antenna is 15.9 dBi at frequency 3 GHz. The measurement is taken under the semi-anechoic chamber and the receiving horn antenna connected with *Anritsu VNA Master* Power meter.
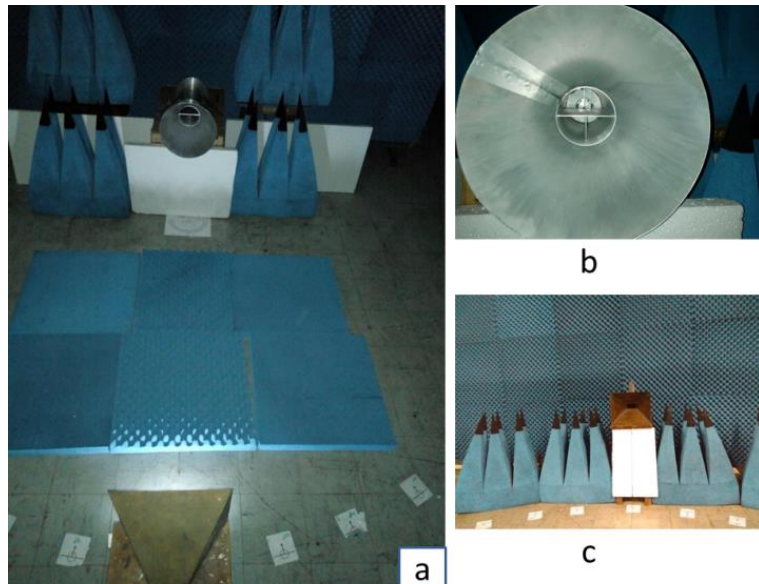

Figure 5.3 (a) Far-field radiation pattern measurement setup, **(b)** fabricated CSWG mode converter, **(c)** receiving horn antenna connected with a power meter.

5.3. Results and Discussion

5.3.1 Simulation

The proposed mode converter is designed and simulated using *CST Microwave Studio*. Aluminium is chosen for the metal with plate thickness 2 mm and cylinder thickness 5 mm. Axial propagation constant is calculated at 3GHz for $CSWG_\pi$ and $CSWG_{\pi/2}$ are $\beta_1(=0.054005)$ and $\beta_2(=0.034942)$, respectively. Using these values in expression (1), the longitudinal length of the metal plate is calculated and its value is $L=165$ mm. The conversion efficiencies from the input TM_{01} mode to other modes are shown in Figure 5.4. The simulated mode conversion efficiency of the mode converter is measured at the end of Region *IV*. Three output modes observed are TE_{11}, TE_{21}, and TM_{01}, with some significant values. As shown in Figure 5.4, at 3 GHz the conversion efficiency of TE_{11} is 92.32%, TE_{21} is 0.69% and TM_{01} is 6.00%. The total radiated power is 99.01% of the input power, which can be further directed at a point or plane at the far-field by using proper RF windowing. The conversion efficiency of this mode converter is more than 90% over the frequency range 2.97-3.02GHz and the total power transferred more than 90% of input power over the frequency range 2.89-3.04GHz.
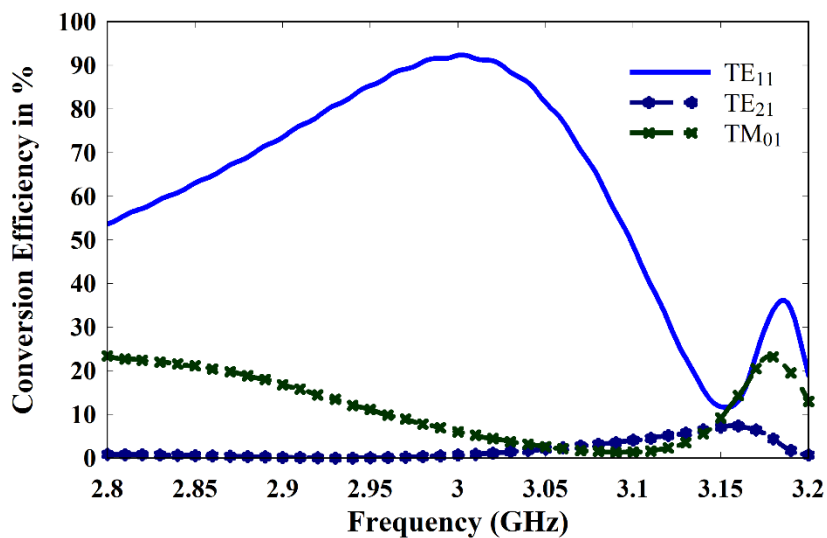

Figure 5.4. The simulated conversion efficiency of the mode converter for the TM_{01} mode to other modes at the output port.

85

5.3.2   *Power Handling Capability*

Power handling capability is obtained by simulating the mode converter model with the 500 MW level signal at the input port of the mode converter. At 1-atm air pressure is used as a medium, the maximum electric field inside the mode converter is 93.3 kV/mm, as shown in Figure 5.5. The field values are within the breakdown limit of 100 kV/mm [Chittora *et al.* (2015) and Zhang *et al.* (2014)] Therefore the proposed mode converter has the ability to use for HPM systems at mega-watt level.
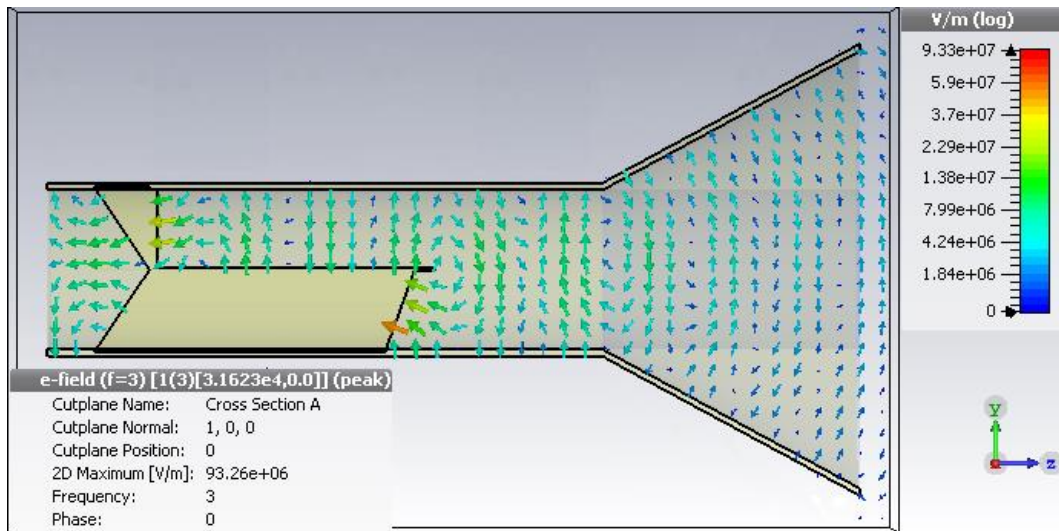

Figure 5.5. At 500MW power E field pattern on the x=0 plane, for CSWG mode converter.

5.3.3   *Experimental Analysis*

The excitation of mode converter is achieved by connecting the mode launcher. Its ability of mode conversion from *TEM* mode to TM_{01} mode is high as required and is shown in Figure 5.6, in the form of *S* parameter.
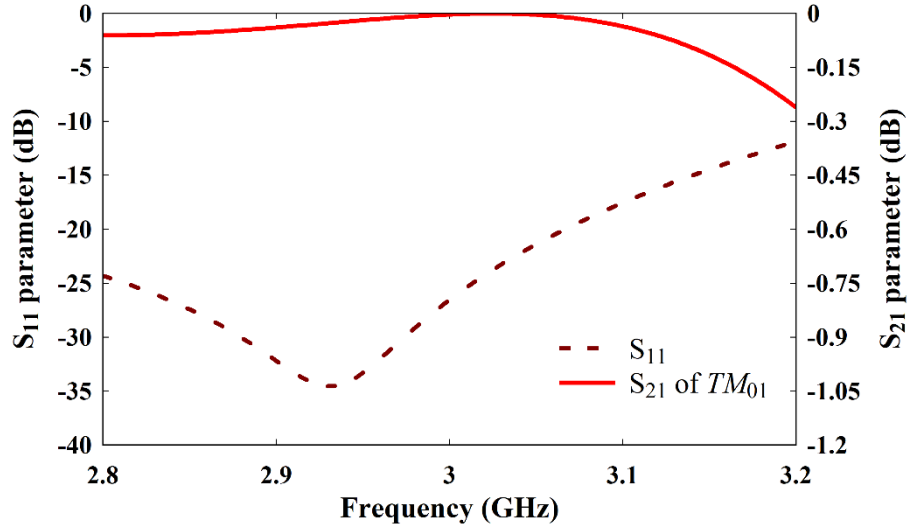
Figure 5.6. *S* parameter results of mode launcher.

In order to verify the proposed design performance, the mode converter is simulated using *CST Microwave Studio* Time Domain solver. Using 15 cells per wavelength at 1-atm air pressure and excitation signal amplitude 31.62 kV simulation is performed. The reflection parameter results indicate that return loss is -19.79 dB at the 3 GHz frequency. While the measured results indicate a high return loss that is -22.48 dB at the same frequency as shown in Figure 5.7.
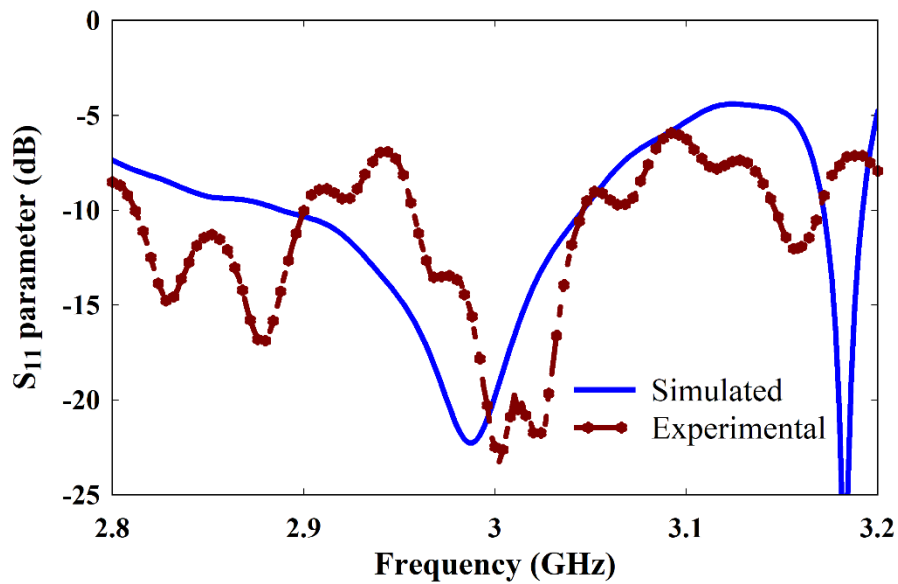

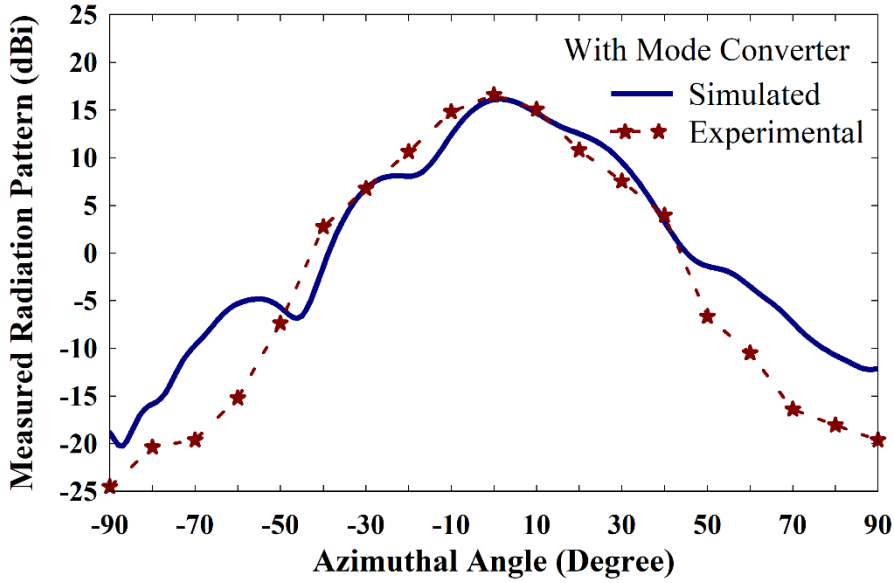**Figure 5.7.** *S* parameter results of the mode converter

Figure 5.8. Radiation pattern results for E plane.

The far-field radiation pattern is shown in Figure 5.8 and shows a good agreement between simulated and measured results. The radiation pattern shows the characteristic of the TE_{11} mode in both simulated and measured graph. From the angle 0° left part of the radiation pattern is not symmetrical, due to unequal power distributed in between $CSWG_{\pi}$ and $CSWG_{\pi/2}$.

5.3.4   *Comparison of Weight*

The mode converter design proposed in Chapter 3 (SWG mode converter) contains a heavy inner coaxial conductor and the mode converter design proposed in this chapter (CSWG mode converter) is only having metallic plates. SWG mode converter has the advantage of high HPM capability and the design has been filled with vacuum can have a maximum electric field 61.87 MV/m, whereas CSWG mode converter design has the maximum electric field 93.3 kV/mm and comparatively low HPM capability. Also, the convergence efficiency SWG mode converter is 98.42% and CSWG mode converter conversion efficiency of TE_{11} is 92.32%, TE_{21} is 0.69% and TM_{01} is 6.00% and the total radiated power of the input power is 99.01%. This shows that the utility of both mode

88

converter in HPM system. As shown in Figure 5.9, the weight of the SWG mode converter is 5.48 Kg, and the CSWG mode converter weight is only 2.30 Kg, which is less than half of the SWG mode converter and is beneficial in low weight application. So in the space program and in designing low weight compact defence equipment; the utility of the low weight mode converter is in advantage. In future by using proper RF windowing the radiated RF beam of CSWG mode converter could converge and this can make it more utilitarian in many applications.

Figure 5.9. Weight of **(a)** SWG mode converter (reported in Chapter 3), **(b)** CSWG mode converter.

5.4. Conclusions

This Chapter presents a cylindrical SWG mode converter design to convert TM_{01} mode to TE_{11} mode. The conversion efficiency of this mode converter is found to be more than 90% over the frequency range of 2.97-3.02 GHz and the total power transferred more than 90% of input power over the frequency range 2.89-3.04 GHz. This mode converter has exhibited ability to use for the HPM systems at Mega-watt level

microwave power. The proposed mode converter is lower in weight with high return loss. The other advantages are a linear, compact structure and High Power handling capability. In future, such design can be studied to keep the HPM system thermally stable for the improved system performance.